Supplementary Data

Electrochemical redox *in-situ* welding of silver nanowire films with high transparency and conductivity

*Wang Zhang, Jia-Shuan Bao, Chen-Hui Xu, Peng-Feng Zhu, Xiang-Liang Pan, and Rui Li**

1. Supplementary figures

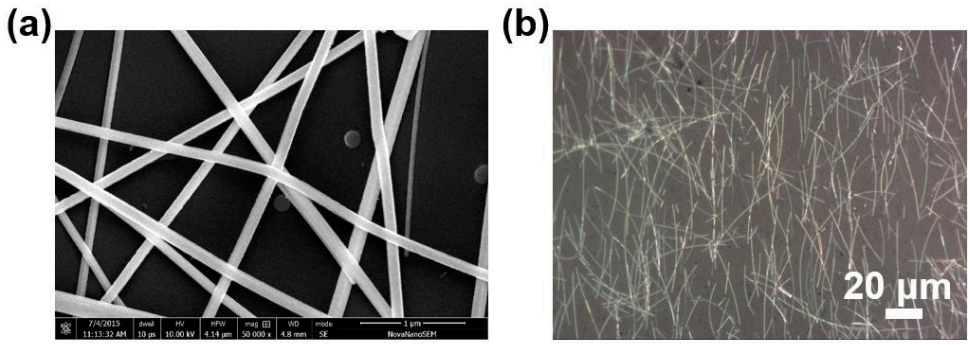

Fig. S1. a) SEM and b) optical microscope images of AgNWs

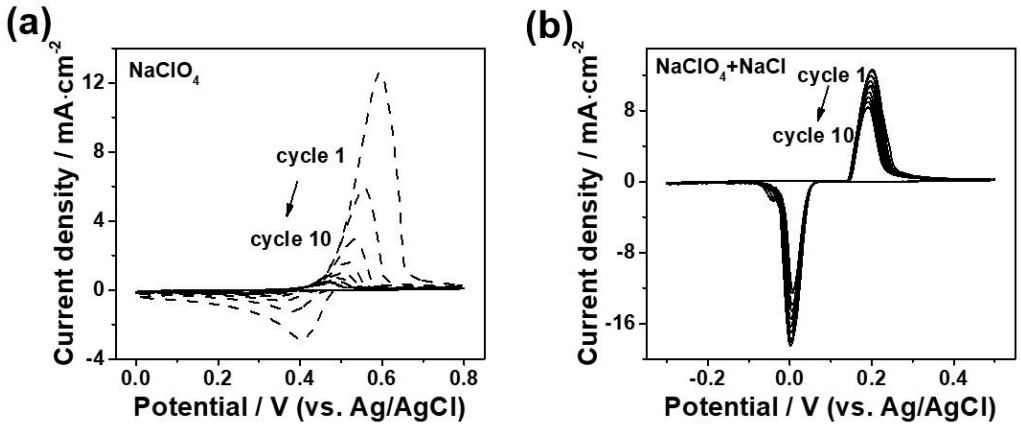

Fig. S2. CV curves of AgNWs with a scan rate of 100 mV s^{-1} in a N_2-saturated 0.5 M $NaClO_4$ without (a) and with (b) 0.1 M NaCl.

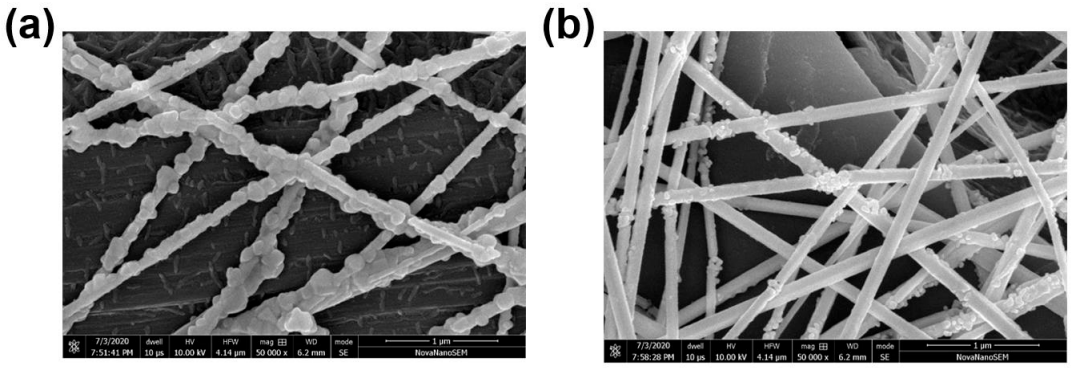

Fig. S3. SEM images of AgNWs/CP-Ox (a) and AgNWs/CP-Re (b).

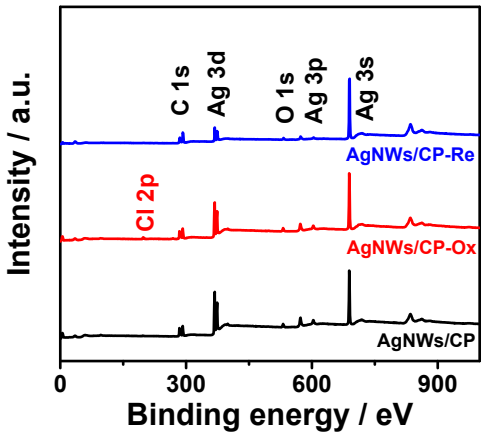

Fig. S4. XPS survey spectra of AgNWs/CP, AgNWs/CP-Ox and AgNWs/CP-Re.

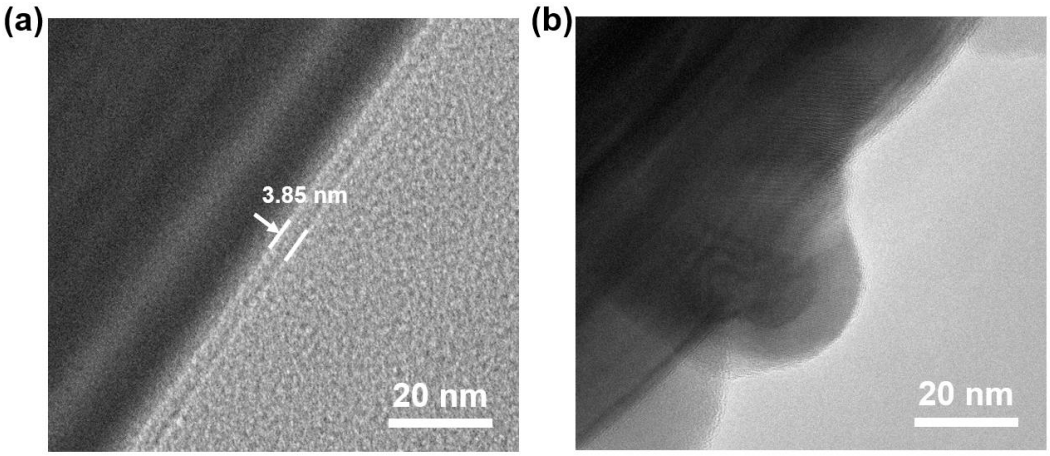

Fig. S5. TEM images of pristine AgNWs (a) and oxidated AgNWs (b).

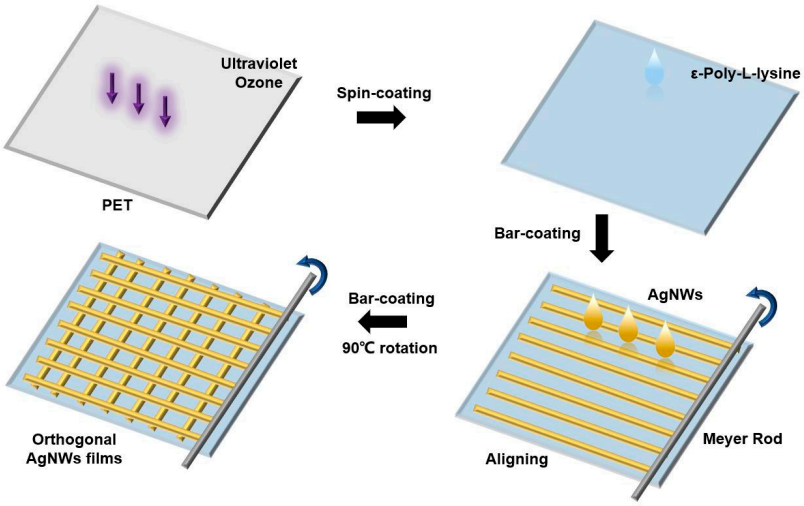

Fig. S6. Schematic illustration of the fabrication of cross-aligned AgNW-TCFs.

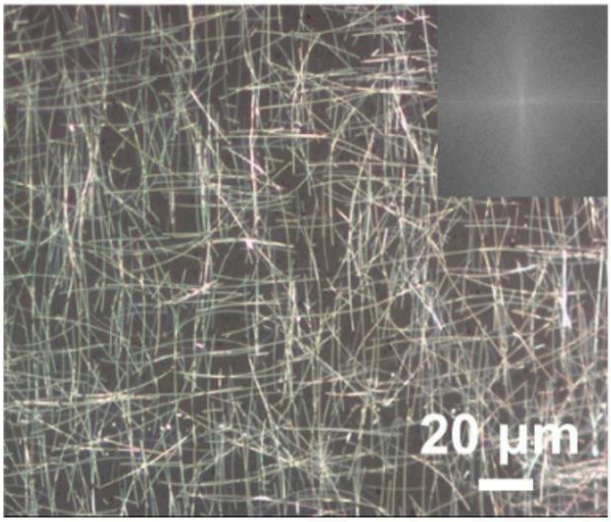

Fig. S7. Optical microscope image of a cross-aligned AgNW-TCF. Inset is the fast Fourier transform analyses, showing the orientation and uniformity of the aligned AgNWs.

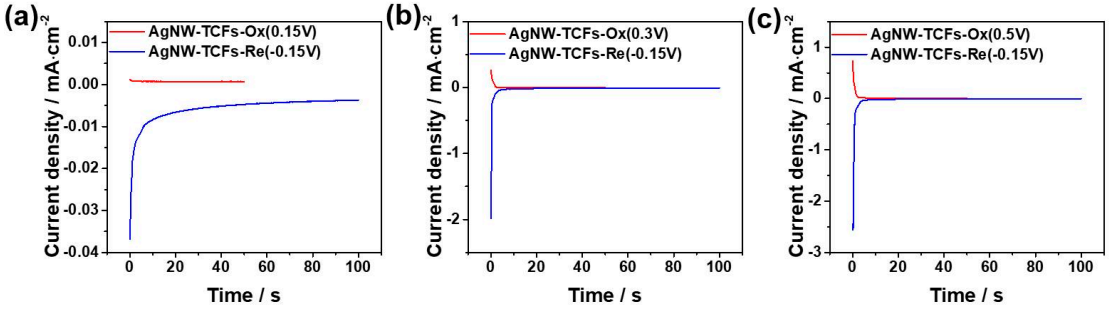

Fig. S8. Polarization curves of AgNW-TCFs under different oxidation potentials at 0.15 V (a), 0.3 V (b) and 0.5 V (c) (vs. Ag/AgCl) for 50 s and the same reduction potential at -0.15 V (vs. Ag/AgCl) for 100 s.

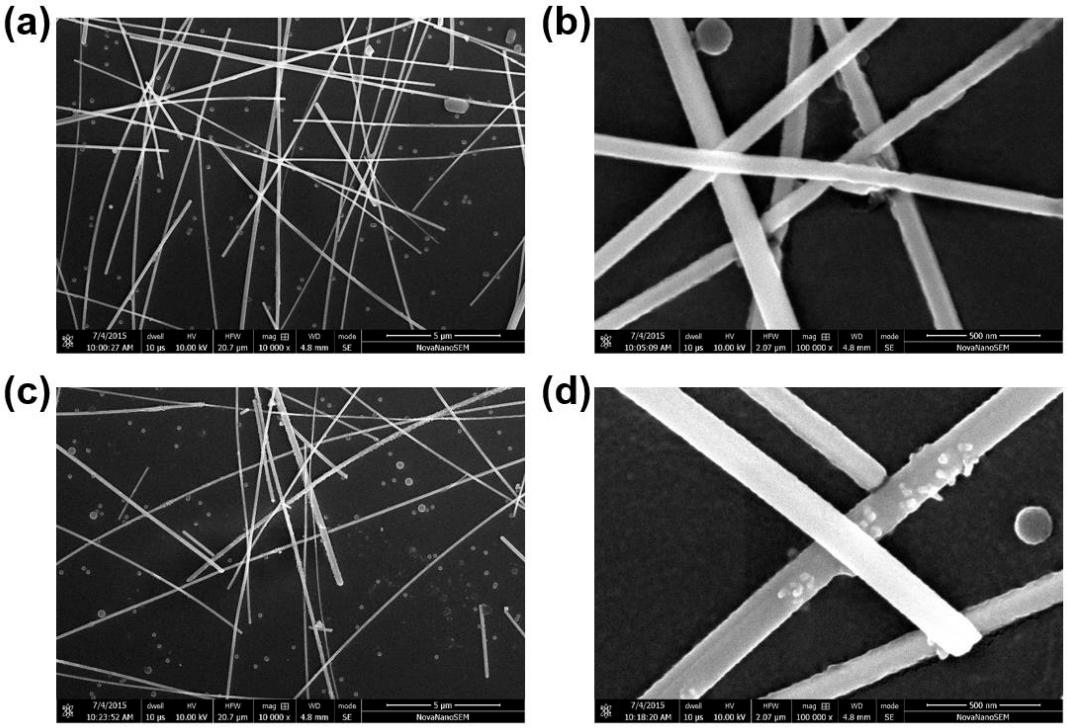

Fig. S9. SEM images of AgNW-TCFs oxidated at 0.15 V (vs. Ag/AgCl) (a,b) and reduced at -0.15 V (vs. Ag/AgCl) (c,d).

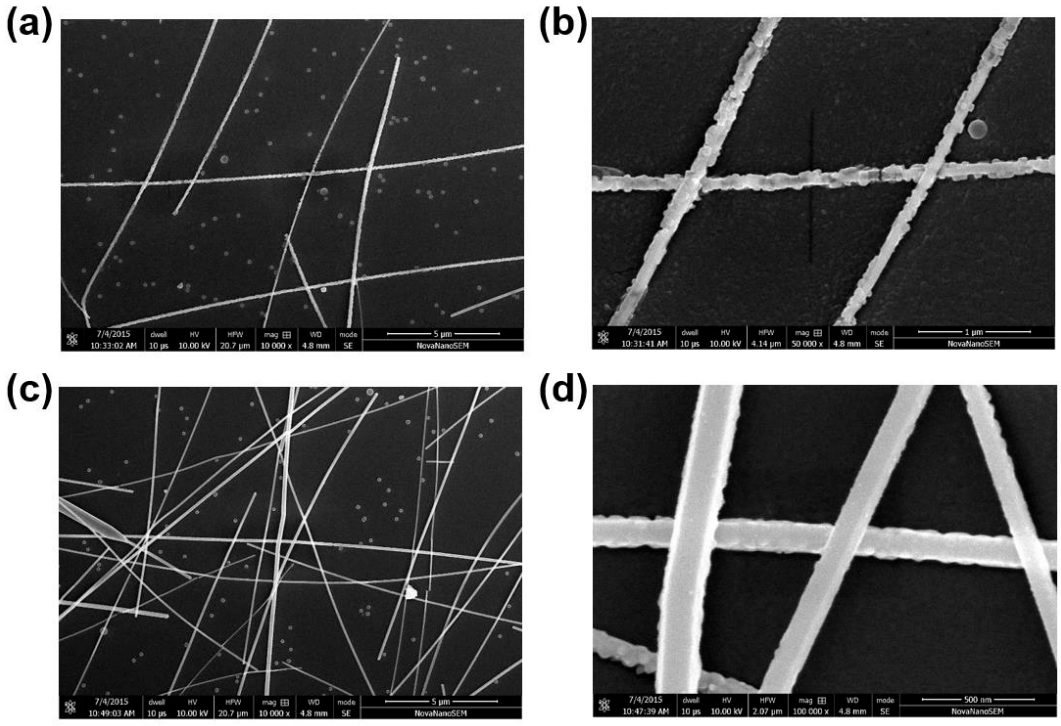

Fig. S10. SEM images of AgNW-TCFs oxidated at 0.3 V (vs. Ag/AgCl) (a,b) and reduced at -0.15 V (vs. Ag/AgCl) (c,d).

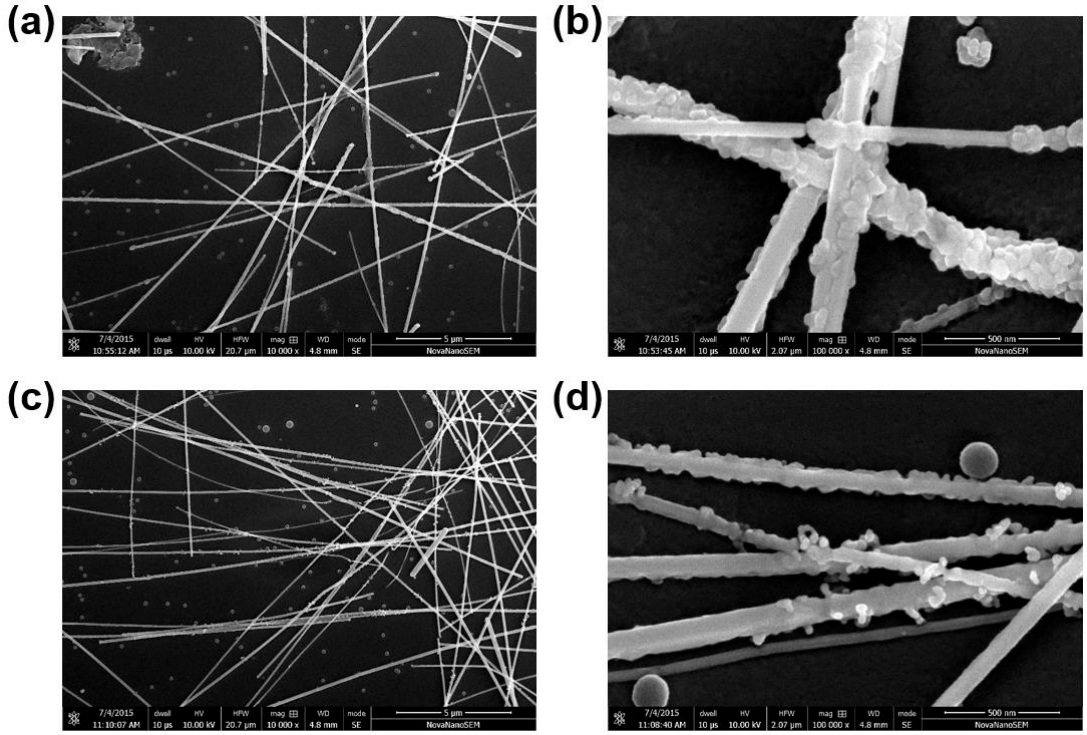

Fig. S11. SEM images of AgNW-TCFs oxidated at 0.5 V (vs. Ag/AgCl) (a,b) and reduced at -0.15 V (vs. Ag/AgCl) (c,d).

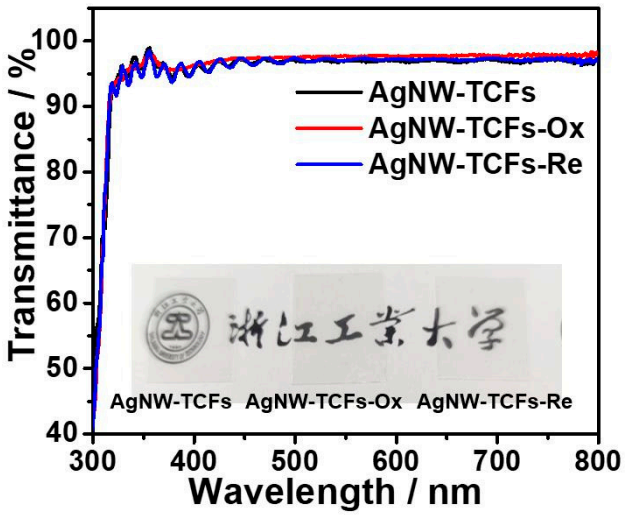

Fig. S12. UV−vis spectra and optical photographs of AgNW-TCFs, AgNW-TCFs-Ox and AgNW-TCFs-Re.

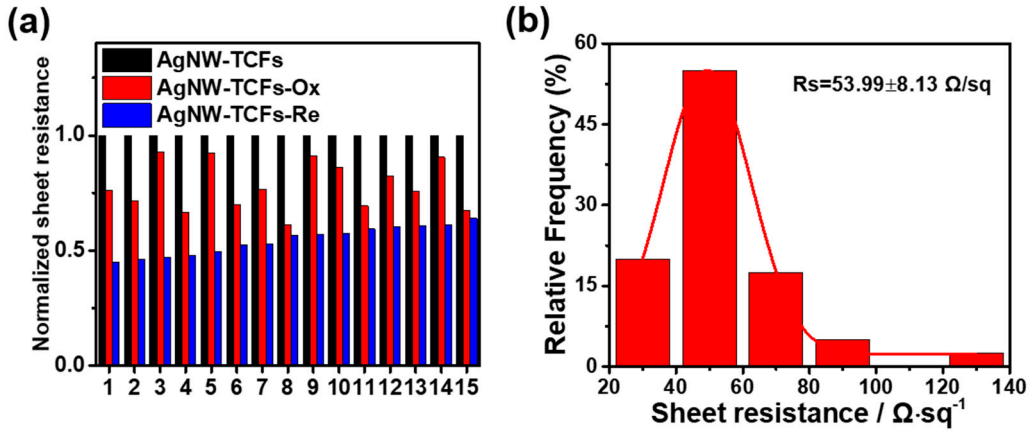

Fig. S13. Normalized sheet resistance of AgNW-TCFs, AgNW-TCFs-Ox and AgNW-TCFs-Re for comparing (a); The frequency distribution histogram of sheet resistance for AgNW-TCFs-Re (b).

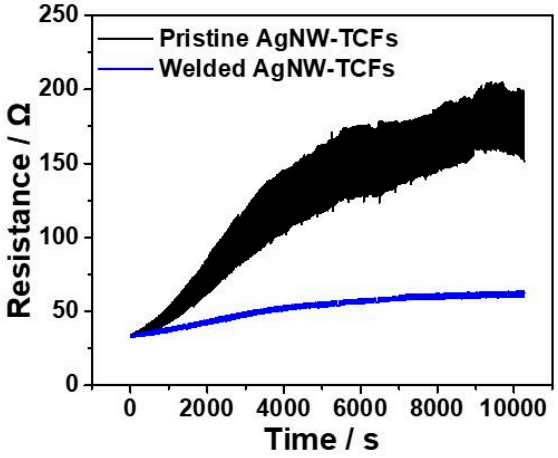

Fig. S14. Time-dependent resistance variation for the pristine and welded AgNW-TCFs.

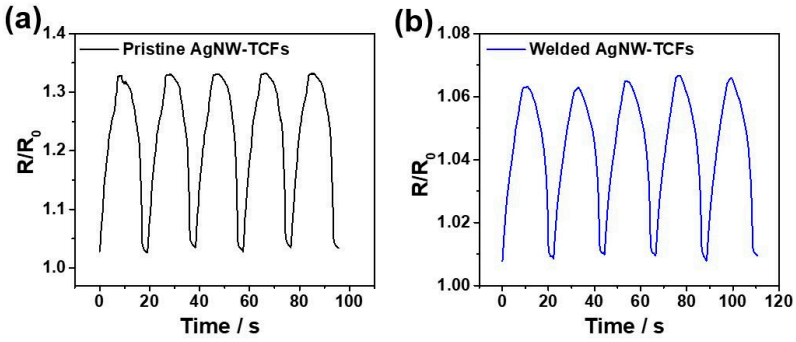

Fig. S15. Plots of relative resistance variation (R/R_0) as a function of time for the pristine (a) and welded AgNW-TCFs (b).

2. Supplementary tables

Table S1. Comparing of sheet resistance for AgNW-TCFs, AgNW-TCFs-Ox and AgNW-TCFs-Re.

Sample	Sheet resistance (Ω/sq)			
	AgNW-TCFs	**AgNW-TCFs-Ox**	**AgNW-TCFs-Re**	**$\Delta R/R_0$**
1	114.7	87.5	51.72	-54.91%
2	70	50.16	32.37	-53.76%
3	87.5	81.3	41.16	-52.96%
4	108.4	72.39	52.01	-52.02%
5	144	133.3	71.24	-50.53%
6	135.43	94.6	71.23	-47.41%
7	131	100.4	69.27	-47.12%
8	73.6	44.98	41.57	-43.52%
9	91.7	83.5	52.44	-42.81%
10	90.34	77.9	51.83	-42.63%
11	115.6	80.3	68.64	-40.62%
12	151.86	125.1	91.99	-39.42%
13	52.77	39.92	32.03	-39.30%
14	55.61	50.36	34.1	-38.68%
15	103.9	69.9	66.4	-36.09%

Table S2. Electrical properties at five data points in a CAFM deflection image of AgNW-TCFs, AgNW-TCFs-Ox and AgNW-TCFs-Re.

Electrical Property	Sample	I	II	III	IV	V	Average
Conductivity ($\mu A\ V^{-1}$)	AgNW-TCFs	632	631	642	644	640	638
	AgNW-TCFs-Ox	681	675	683	674	674	677
	AgNW-TCFs-Re	832	833	839	838	841	837
Resistance (Ω)	AgNW-TCFs	1580	1580	1560	1550	1560	1570
	AgNW-TCFs-Ox	1470	1480	1460	1480	1480	1470
	AgNW-TCFs-Re	1200	1200	1190	1190	1190	1190